JCTC Journal of Chemical Theory and Computation

ARTICLE

pubs.acs.org/JCTC

Critical Examination of Explicitly Time-Dependent Density Functional Theory for Coherent Control of Dipole Switching

Shampa Raghunathan* and Mathias Nest

Theoretische Chemie, Technische Universität München, Lichtenbergstrasse 4, 85747 Garching, Germany

ABSTRACT: We compare the performance of explicitly time-dependent density functional theory (DFT) with time-dependent configuration interaction (TDCI) to achieve the control task of a population inversion in LiCN. We assume that if a given pulse achieves the control task when used in TDCI, then there should be a pulse with similar frequency and intensity that achieves the task in time-dependent DFT (TDDFT). The present investigation indicates that this is not the case, if standard functionals are used in the adiabatic approximation.

1. INTRODUCTION

Time-dependent density functional theory (TDDFT)[1] is one of the most successful and popular approaches for the calculation of excited-state properties of molecules, as well as to describe the real-time (RT) dynamics of many electron systems. Its computational efficiency has made it one of the first electronic structure methods (after time-dependent Hartree−Fock, TDHF[2]) to be generalized to the real-time domain.[3,4] Much experience about the strengths and limitations of TDDFT has been gained through applications to a wide range of phenomena. Rubio et al.[5] studied as diverse processes as high harmonic generation, Coulomb explosion, and laser-induced photodissociation. The same group also developed the real-space code Octopus,[6−8] one of the most widely used implementations of TDDFT. Other successful applications were to the nonlinear dynamics of electrons in metal clusters[9,10] and molecules.[11−14] Less satisfactory were attempts to describe the nonsequential double ionization of atoms such as He or Ne, especially with respect to the famous "knee" structure in the yield as a function of laser fluence.[15,16] There are various reasons for this mixed success of explicitly time-dependent DFT. First of all, there is the so-called adiabatic approximation;[17] i.e., the time-dependent density $\rho(t)$ is inserted into standard ground-state exchange-correlation (xc) functionals. Obviously, there is no guarantee that these functionals will generate the correct dynamics, although they have been found to be useful in a number of applications mentioned above. Also, some authors have argued that a proper density functional for quantum dynamics should contain a memory term.[18−21] These problems have not yet been fully solved, so that most work is being done using the adiabatic approximation mentioned above. Recently, some significant progress[22] has been made to combine TDDFT with coherent control, or more precisely quantum optimal control theory.[23−25]

In this paper, we want to study the suitability of TDDFT for a simple control task: a state-to-state transition using a so-called π-pulse. An estimate of the necessary laser pulse parameters can be obtained from a configuration interaction (CI) calculation, described in the following sections. Our test molecule will be LiCN, because this has been used in a similar study before.[26,46,47] It also has the advantage that the transition is accompanied by a strong change in the dipole moment, which can serve as a criterion when comparing TDCI[27−29] and TDDFT calculations. If TDDFT provides a correct description of the correlated electron dynamics, then a pulse similar to the one that worked for TDCI should also work for TDDFT. Similarity between laser pulses is defined here as having a similar carrier frequency and intensity. The pulse duration and carrier-envelope phase will be kept fixed.

In section 2 we give some computational details of our simulations and discuss the extent of deviations of molecular properties of LiCN if different electronic structure methods are used. Section 3 presents the main results of this work, and section 4 concludes the paper. Atomic units will be used if not stated otherwise.

2. COMPUTATIONAL DETAILS

The TD Kohn−Sham (KS) equations are given by

$$i\frac{\partial\varphi_i(\mathbf{r},t)}{\partial t} = \left[-\frac{\nabla^2}{2} + v_{\mathrm{eff}}[\rho(t)]\right]\varphi_i(\mathbf{r},t) \tag{1}$$

where the effective potential

$$v_{\mathrm{eff}}[\rho(t)](\mathbf{r},t) = v_{\mathrm{ext}}(\mathbf{r},t) + v_{\mathrm{H}}[\rho(t)](\mathbf{r},t) + v_{\mathrm{xc}}[\rho(t)](\mathbf{r},t) \tag{2}$$

consists of external v_{ext}, Hartree v_{H}, and exchange-correlation v_{xc} contributions. The external potential contains the electron−nuclear attraction and the laser−electron interaction in the dipole approximation

$$v_{\mathrm{ext}}(\mathbf{r},t) = v_{\mathrm{Ne}}(\mathbf{r}) - \boldsymbol{\mu}\mathbf{f}(t)\cos[\omega(t-t_{\mathrm{p}})] \tag{3}$$

with the envelope

$$\mathbf{f}(t) = \begin{cases} \mathbf{f}_0 \cos^2\left[\dfrac{\pi}{2\sigma}(t-t_{\mathrm{p}})\right] & \text{if } |t-t_p| < \sigma \\ \mathbf{0} & \text{else} \end{cases} \tag{4}$$

Received: April 19, 2011
Published: June 24, 2011

dx.doi.org/10.1021/ct200270t | J. Chem. Theory Comput. 2011, 7, 2492–2497

Here, t_p is the time at which the pulse is maximal, σ is the full width at half-maximum (fwhm), and $\mathbf{f}_0$ is the polarization and maximum pulse amplitude.

We performed TDDFT calculations using the program packages Octopus[6,7] and Parsec,[30,31] both of which employ a real-space uniform grid representation using the finite difference approach. For the real-space grid, a simulation sphere of radius 8 a_0, and a grid spacing of 0.4 a_0 are used except for exact-exchange optimized effective potential (OEP-X) calculations, where the radius of simulation sphere was 15 a_0 and the grid spacing was 0.7 a_0. In all calculations, we used norm-conserving, nonlocal, ionic Troullier−Martins[32] pseudopotentials to model the interactions of valence electrons with core electrons. In this scheme, the 1s shells of all three atoms Li, C, and N were treated as the core. In the density functional calculations using the program Parsec, we employed the xc functionals according to the local-density approximation (LDA) with the Perdew−Zunger parametrization[33,34] (CA-PZ), and generalized gradient approximation (GGA) of Perdew−Burke−Ernzerhof (PBE).[35] We further carried out GGA-PBE, and hybrid-DFT PBE0,[36] extended hybrid functional combined with Lee−Yang−Parr correlation functional (X3LYP),[37] and OEP-X calculations using the program Octopus.

The TDKS equations (eq 1) are solved by direct numerical integration in real time. For this purpose, Parsec[38] uses a fourth-order Taylor approximation, whereas Octopus uses an exponential midpoint rule combined with the Lanczos exponential approximation.[39] We have used an electronic time step of 0.24 as (0.01 au) with a total propagation time of 50 fs, and an x-polarized laser pulse has been employed throughout unless stated otherwise.

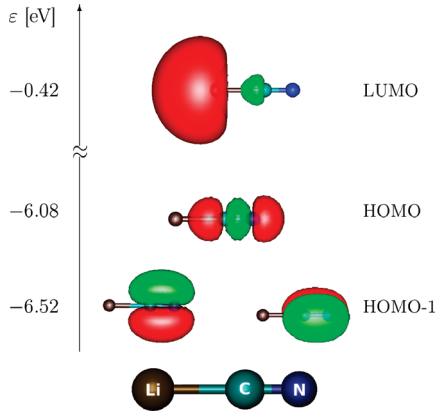

Figure 1. HOMO-1, HOMO, and LUMO molecular orbitals of LiCN along with their orbital energies computed at the GGA-PBE level using Parsec.

Because we want to compare different explicitly time-dependent methods, we will present first some molecular properties from time-independent calculations, like CIS and linear response (LR)-TDDFT and LR-TDHF, in order to assess how much these values change from one method to another. We computed the dipole moments of the ground and selected excited states of LiCN along with the corresponding transition dipole moments and excitation energies. For the LR-TDDFT calculations we employed LSDA,[40] PBE, and PBE0 xc functionals using Gaussian 09.[41] We also performed more accurate correlated calculations such as CISD (10,15) (all singles, doubles restricted to a (10,15) active space) using our own code,[42,43] and EOM-CCSD calculation using the program Molpro.[44] The former, somewhat unusual method is included, because in a later section we report time-dependent results on this level of theory. In all of the above calculations we employed the polarized double-ζ basis set 6-31G*.[45]

From the study of Klamroth et al.,[26] we adopted the equilibrium geometry of LiCN; i.e., $r_{Li-C} = 3.683a_0$ and $r_{C-N} = 2.168a_0$ (with orientation along the z-axis). For the ground-state electronic configuration, the HF method predicted the HOMO to be doubly degenerate $C(2p_{x/y})-N(2p_{x/y})$ π-type MOs and the penultimate MO (i.e., HOMO-1) to be a $C(2p_z)-N(2p_z)$ σ-type MO. On the other hand, in the Kohn−Sham DFT calculations, this order is reversed and the σ-type MO forms the HOMO except for OEP-X calculation, where, the HF ordering of ground-state MOs is preserved. This trend in the ordering of the occupied MOs in DFT calculations has been predicted by both grid-based and basis set approaches. Both in HF and DFT approaches the LUMO is essentially the Li (2s) orbital with a weak σ^* character; see Figure 1.

Table 1 summarizes dipole moments, transition dipole moments, and the excitation energies. The transition we are interested in, $CN(\pi) \rightarrow Li(\sigma^*)$, is from the ground state (S_0) to the second or third excited states of LiCN (S_2 or S_3). These degenerate states can be accessed selectively by laser pulses polarized along the x or y direction. A complete population transfer to these excited states will switch the z-component of the dipole moment from $\mu_{0,0;z} \approx -3.5\ ea_0$ to $\mu_{2(3),2(3);z} \approx +2\ ea_0$, with comparatively small deviations between various quantum chemical methods. In all our LR-TDDFT calculations, done using Gaussian 09,[41] the permanent dipole moments, $\mu_{0,0;z}$ and $\mu_{2(3),2(3);z}$, are predicted to be in good agreement with the EOM-CCSD values; however, the transition dipole moments are

Table 1. Selected Ground- and Excited-State Properties of LiCN Computed Using Linear Response (LR) Theories along with EOM-CCSD[a]

methods	$\mu_{0,0;z}$	$\mu_{2(3),2(3);z}$	$\mu_{0,2;x}$	$\mu_{0,2;y}$	$\mu_{0,3;x}$	$\mu_{0,3;y}$	$\Delta E_{0\rightarrow 2(3)}$
LR-HF[b]	−3.7080	1.8329	0.2682	0.1503	0.1503	−0.2682	6.57
CIS[b]	−3.7080	1.8450	0.3075	0.0258	0.0258	−0.3075	6.58
CIS(D)[c]	−3.7082	2.7952	0.3084	0.0095	0.0095	−0.3084	6.13
CISD(10,15)[d]	−3.4662	1.8338	0.2981	0.0902	0.0902	−0.2981	6.77
EOM-CCSD[e]	−3.5502	2.0315	0.3833	0.0	0.0	−0.3833	6.28
LR-LSDA[b]	−3.4193	2.2172	0.2675	0.0933	0.0933	−0.2675	4.77
LR-PBE[b]	−3.3951	2.1553	0.2442	0.0890	0.0890	−0.2442	4.31
LR-PBE0[b]	−3.5114	2.0748	0.2628	0.0123	0.0123	−0.2628	5.13

[a] Ground- and excited-state dipoles, transition dipole moments ($\mu_{i,j;q}$, ea_0) and excitation energies (ΔE, eV) are given. [b] Using Gaussian 09. [c] From ref 26. [d] Own code. [e] Using Molpro.

dx.doi.org/10.1021/ct200270t |J. Chem. Theory Comput. 2011, 7, 2492–2497

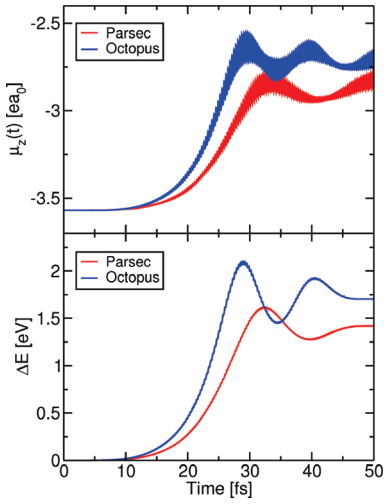

Figure 2. Time evolution of dipole moments and energies computed at the GGA-PBE level using Parsec and Octopus programs: dipole signal of LiCN upon laser excitation (top); time-dependent relative energy (with respect to ground electronic state energy at t = 0 fs) (bottom). ω = 6.3 eV, field strength 0.004 928 E_h/ea_0 polarized along x,and total propagation time = 50 fs.

slightly underestimated to lie in the range of 0.244−0.268 ea_0, close to the LR-TDHF value.

Before we present results of our quantum dynamical calculations, it is worthwhile also to compare the different implementations of TDDFT in Parsec and Octopus. We do so by showing the excitation energy and dipole moment of LiCN computed using these two programs at the GGA-PBE level with a laser frequency (ω) of 6.3 eV and a field strength of 0.004 928 E_h/ea_0; see Figure 2. Although the results are qualitatively the same, they are not identical. The size of the grid, the grid spacing, and the pseudopotentials were the same in both programs. We can only speculate that internal differences in either the propagation scheme or the treatment of the Coulomb singularity are responsible for the differences, which become amplified by the nonlinearity of the equations of motions. Alternatively, a bug in one of the implementations cannot be ruled out completely.

3. RESULTS

3.1. Dipole Switching. The full population inversion from the ground to the second excited state can be achieved by a π-pulse. For laser pulses with a $\cos^2$ envelope, the condition for the amplitude is

$$|\mathbf{f}_0| = \frac{\pi}{\sigma|\mu_{i,j;q}|} \tag{5}$$

where $\mu_{i,j;q}$ is the transition dipole moment between states i and j, and q indicates the polarization. Also, a π-pulse requires that the laser pulse is long enough to be resonant with the desired transition and that no energetically close states are present which have a significant transition dipole moment, too. Using this condition for TDCIS and TDCISD(10,15), together with the information from Table 1, we achieve a controlled switching of the z-component of the dipole moment and excitation energies; see Figure 4. Because the transition dipole moments are similar for both methods, the pulses are similar too, and they can serve as a starting point when looking for laser pulses suitable for TDDFT. The total propagation time is 50 fs, or σ = 25 fs in eq 4.

The π-pulse condition can be readily applied to TDCI calculations, because a time-independent many-body basis exists. In other words, the Slater determinants made of Hartree−Fock orbitals span always the same Hilbert space. It has been shown already for MCTDHF[48−50] that a time-dependent basis leads to a time-dependent electronic structure, making the concept of a resonant transition questionable. Moreover, the linear-response values of TDDFT given in Table 1 cannot easily be translated to the explicitly time-dependent, nonlinear regime. On the other hand, if TDDFT provides a realistic approximation to the true dynamics of the system, then a pulse similar to those used in TDCI should perform a similar task. Looking for this "similar pulse", we pursued the following strategy for a variety of density functionals. First, we scanned a range of laser frequencies (ω) between 4.9 and 6.5 eV (4−7 eV for PBE). We identified promising frequencies, to which the system reacts strongly, which indicates proximity to a resonance. For the two TDCI based methods this is simply the excitation energy given in Table 1, whereas TDDFT calculations show the resonances at 6.1, 6.3, 5.3, 5.5, and 6.1 eV using the xc functionals LDA, PBE, PBE0, X3LYP, and OEP-X, respectively, and for TDHF ω = 6.9 eV. Next, an optimal field strength has to be found. This posed a somewhat bigger problem, because several criteria could be applied. On the one hand, the dipole switching as described by TDCI is a one-photon absorption process. On the other hand, one would like to achieve a final state, which is as close to stationary as possible. We have attempted both and report the results in the following.

Figure 3 shows the energy uptake and time-dependent dipole moments of LiCN, if the field strengths are adjusted to a one-photon absorption. For TDCIS ($f_{0,x}$ = 0.009 377 E_h/ea_0) and TDCISD(10,15) ($f_{0,x}$ = 0.010 198 E_h/ea_0), the field strengths follow from the π-pulse equation (eq 5), while for TDDFT and TDHF a scan over pulse amplitudes is necessary. For TDDFT calculations the field strengths are 0.0371, 0.0392, 0.0182, 0.021 57, and 0.0261 E_h/ea_0 using the xc functionals LDA, PBE, PBE0, X3LYP, and OEP-X, respectively, and for TDHF $f_{0,x}$ = 0.045 E_h/ea_0. The density functional based methods and Hartree−Fock obviously require a much larger fluence, than the CI based methods. Clearly a multitude of excited states is populated, leading to oscillating wave packets, that have no similarity with dipole switching.

The results obtained from the second criterion, which focuses on stationarity of the dipole moment at late times, are shown in Figure 4. TDCIS and TDCISD(10,15) use the same field strengths as used in the case of one-photon absorption calculations. TDDFT calculations use the field strengths of 0.004 928 E_h/ea_0 for LDA, PBE, and X3LYP functionals and 0.003 and 0.009 856 for PBE0 and OEP-X functionals, and for TDHF $f_{0,x}$ = 0.009 919 E_h/ea_0. The results for all five functionals and HF are qualitatively the same: the dipole moment changes by about 1 ea_0, instead of about 5.5 ea_0 as in TDCI.

How can this failure of real-time TDDFT, using standard functionals in the adiabatic approximation, be explained? It is well-known that linear-response TDDFT has problems describing charge transfer. But, in our case, the charge transfer is only on a small length scale, and is not ameliorated by hybrid functionals. Also the use of exact exchange does not improve the results. To emphasize this point, we included TDHF in the list of methods above. Further, in the LR-TDDFT theory, Tozer and co-workers

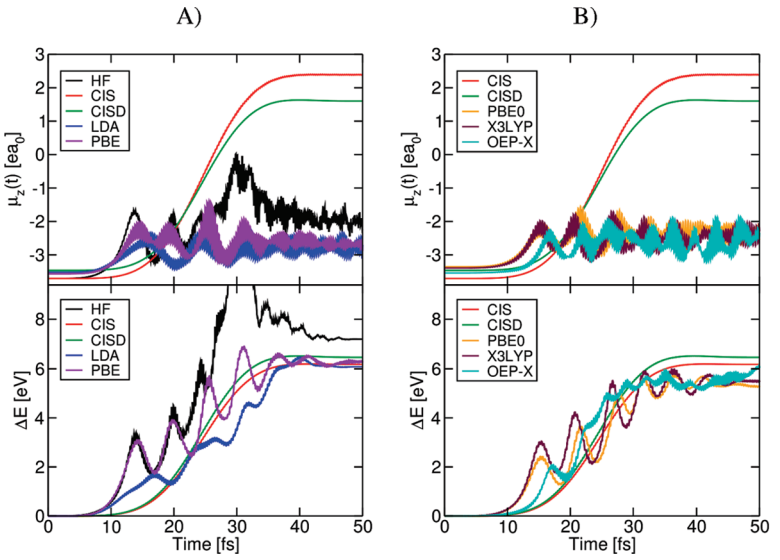

Figure 3. Time evolution of dipole moments and energies for one-photon absorption computed using different theoretical methods: dipole z-component as a function of time (top); time-dependent relative energy (with respect to ground electronic state energy at $t = 0$ fs) (bottom). Laser parameters ($f_{0,x}$ in E_h/ea_0 and ω in eV) for A: (HF) $f_{0,x} = 0.045$, $w = 6.9$; (CIS) $f_{0,x} = 0.009\,377$, $\omega = 6.6$; (CISD) $f_{0,x} = 0.010\,198$, $\omega = 6.8$; (LDA) $f_{0,x} = 0.0371$, $\omega = 6.1$; (PBE) $f_{0,x} = 0.0392$, $\omega = 6.3$. Laser parameters for B, including the same CIS and CISD values: (PBE0) $f_{0,x} = 0.0182$, $\omega = 5.3$; (X3LYP) $f_{0,x} = 0.02157$, $\omega = 5.5$; (OEP-X) $f_{0,x} = 0.0261$, $\omega = 6.1$. Total propagation time = 50 fs.

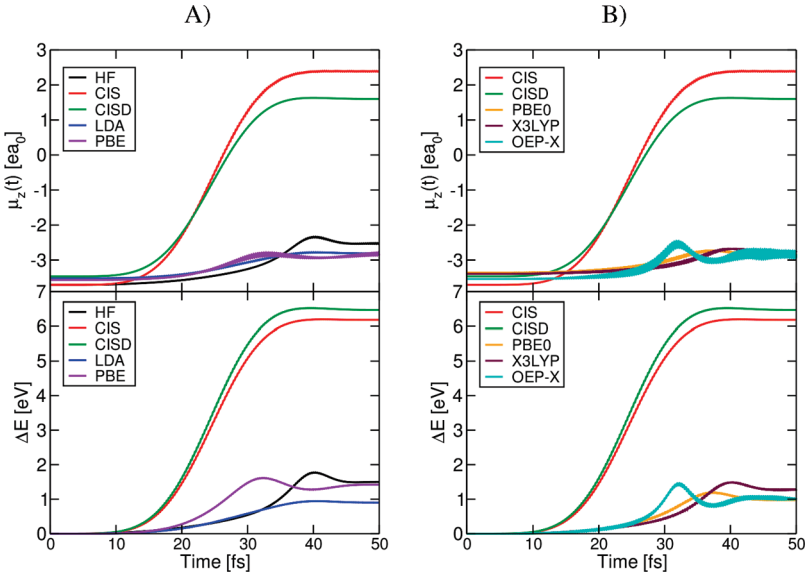

Figure 4. Time evolution of dipole moments and energies computed using different theoretical methods: dipole z-component as a function of time (top); time-dependent relative energy (with respect to ground electronic state energy at $t = 0$ fs) (bottom). Laser parameters ($f_{0,x}$ in E_h/ea_0 and ω in eV) for A: (HF) $f_{0,x} = 0.009\,919$, $\omega = 6.9$; (CIS) $f_{0,x} = 0.009\,377$, $\omega = 6.6$; (CISD) $f_{0,x} = 0.010\,198$, $\omega = 6.8$; (LDA) $f_{0,x} = 0.004\,928$, $\omega = 6.1$; (PBE) $f_{0,x} = 0.004\,928$, $\omega = 6.3$. Laser parameters for B, including the same CIS and CISD values: (PBE0) $f_{0,x} = 0.003$, $\omega = 5.3$; (X3LYP) $f_{0,x} = 0.004\,928$, $\omega = 5.5$; (OEP-X) $f_{0,x} = 0.009\,856$, $\omega = 6.1$. Total propagation time = 50 fs.

proposed[51,52] a weighted overlap parameter which can be considered as an indirect measure for the probability of charge transfer. They suggested that a small overlap indicates less sharing of similar regions of space between the corresponding orbitals involved in the excitation, which restricts the CT excitation. In our study, we simply considered the spatial overlap between the π and σ^* states, $O_{\pi\sigma^*}$, computed as

$$O_{\pi\sigma^*} = \int |\varphi_\pi(\mathbf{r})|\,|\varphi_{\sigma^*}(\mathbf{r})|\,\mathrm{d}\mathbf{r} \qquad (6)$$

For this quantity, $O_{\pi\sigma^*}$, we found a value of 0.18 from LDA-CA-PZ and GGA-PBE calculations which implies a weak overlap between the fragment orbitals CN(π) and Li(σ^*). This is a small value, but probably not small enough to account for the failure of all functionals. The origin of the problem is probably indeed related to the fact that TDDFT and TDHF (as to some degree MCTDHF) use a time-dependent basis. We assume that this leads to an effective time-dependent excitation energy between S_0 and S_2 so that resonant excitation cannot take place. Similar observations have been made with regard to Rabi oscillations by

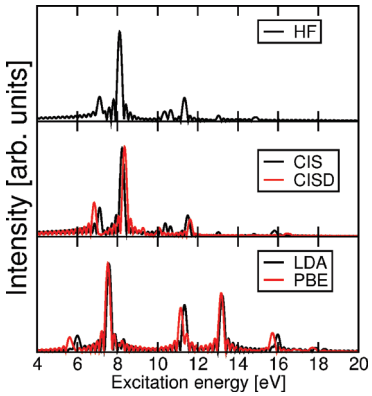

Figure 5. Excitation spectra of LiCN obtained from Fourier transform of $\mu_z(t)$, computed at different explicitly TD theories with a laser pulse of frequency 6.0 eV, $\mathbf{f}_0 = (0.002, 0.002, 0.002)\ E_h/ea_0$, $\sigma = 0.5$ fs, and total propagation time = 20 fs.

other groups.[53,54] The paper of Rubio et al.[53] suggests a new constraint on standard functionals is required to prevent this detuning. It should also be noted that it is quite difficult to quantify by how far the target state has been missed. In this paper we used the energy and dipole moment as measure, but this provides only restricted information. Simulations for model systems, where difference densities and currents can be evaluated much easier are under way. This will also provide insight whether the quantum systems are taking the same "path" from the initial to the final state. While terms such as $\langle S_0 |\boldsymbol{\mu}| S_2\rangle$ in TDCI produce the desired population transfer, there is no analogue when time-dependent orbitals are used. The operation of $\boldsymbol{\mu}$ on an orbital does not guarantee that the orbitals will change in the physically correct way.

3.2. Ultrashort Laser Pulse Excitation. Finally, we discuss a different aspect of the problem at hand. The task in the previous subsection was to populate a state which was orthogonal to the initial ground state. This turned out to be surprisingly difficult but does not say anything about the performance of TDDFT if the perturbation is smaller. Therefore, we excited the LiCN molecule with an ultrashort laser pulse with $\sigma = 0.5$ fs, $\omega = 6$ eV, and a field strength/polarization of $\mathbf{f}_0 = (0.002, 0.002, 0.002)\ E_h/ea_0$. This pulse gives a "kick" to the electron system so that they start to oscillate. We recorded the time-dependent dipole moment for 20 fs and calculated the Fourier transform to obtain the absorption spectrum. Figure 5 shows the excitation energy spectra calculated from $\langle\mu_z\rangle(t)$ for various explicitly time-dependent methods. The TDHF spectrum is almost identical to the TDCIS spectrum, and TDCISD(10,15) shifts the results only marginally. The two TDDFT spectra are superficially similar to those from wave function based methods. The peaks at 6 and 8 eV are both shifted somewhat to lower energies but not more than can be expected if the electronic structure method is changed. Even the relative height of these two dominant peaks is semiquantitatively correct. However, the peaks at higher energies come out too strong. Overall, TDDFT performs rather well in this case. This finding might indicate that there is a relation between the performance of real-time TDDFT with standard functionals and in the adiabatic approximation on one side, and the distance between initial and final states, measured in energy or as a distance in Hilbert space, on the other side.

4. CONCLUSIONS

We compared the performance of explicitly time-dependent DFT with TDCI to achieve the control task of a population inversion in LiCN. We found that no pulse similar to the one used for TDCI will perform the task in TDDFT, if standard functionals and the adiabatic approximation are used. Similarity of pulses is defined here as similarity in laser frequency and field strength. Maybe the introduction of a chirp or a pulse sequence would have allowed TDDFT to achieve the task, but probably for a physically wrong reason. The use of hybrid functionals or exact exchange did not improve the results. This indicates that results obtained from a combination of TDDFT in its standard implementation and coherent control schemes have to be taken with care.

AUTHOR INFORMATION

Corresponding Author
*E-mail: shampa@mytum.de.

ACKNOWLEDGMENT

We thank the Munich Centre for Advanced Photonics for financial support and Michael Mundt for the technical help.

REFERENCES

(1) Runge, E.; Gross, E. K. U. *Phys. Rev. Lett.* **1984**, *52*, 997.
(2) Kulander, K. C. *Phys. Rev. A* **1987**, *36*, 2726.
(3) Ullrich, C. A.; Erhard, S.; Gross, E. K. U. In *Super Intense Laser Atom Physics IV*; Muller, H. G., Fedorov, M. V., Eds.; Nato Advanced Study Institutes, Ser. 3; Kluwer: Dordrecht, The Netherlands, 1996; Vol. 13, p 267.
(4) Calvayrac, F.; Reinhard, P.-G.; Suraud, E. *Phys. Rev. B* **1995**, *52*, R17056.
(5) Castro, A.; Marques, M. A. L.; Alonso, J. A.; Bertsch, G. F.; Rubio, A. *Eur. Phys. J. D* **2004**, *28*, 211.
(6) Marques, M. A. L.; Castro, A.; Bertsch, G. F.; Rubio, A. *Comput. Phys. Commun.* **2003**, *151*, 60.
(7) Castro, A.; Appel, H.; Oliveira, M.; Rozzi, C. A.; Andrade, X.; Lorenzen, F.; Marques, M. A. L.; Gross, E. K. U.; Rubio, A. *Phys. Status Solidi B* **2006**, *243*, 2465.
(8) http://www.tddft.org/programs/octopus.
(9) Calvayrac, F.; Reinhard, P.-G.; Suraud, E.; Ullrich, C. A. *Phys. Rep.* **2000**, *377*, 493.
(10) Fennel, Th.; Meiwes-Broer, K.-H.; Tiggesbäumker, J.; Reinhard, P.-G.; Dinh, P. M.; Suraud, E. *Rev. Mod. Phys.* **2010**, *82*, 1793.
(11) Chu, X.; Chu, S. *Phys. Rev. A* **2001**, *64*, 063404.
(12) Suzuki, Y.; Seideman, T.; Stener, M. *J. Chem. Phys.* **2004**, *120*, 1172.
(13) Remacle, F.; Levine, R. D. *Proc. Natl. Acad. Sci. U. S. A.* **2006**, *103*, 6793.
(14) Remacle, F.; Levine, R. D. *J. Phys. Chem. C* **2007**, *111*, 2301.
(15) Lappas, D. G.; van Leeuwen, R. *J. Phys. B* **1998**, *31*, L249.
(16) Bauer, D.; Ceccherini, F. *Opt. Express* **2001**, *8*, 377.
(17) Gross, E. K. U.; Burke, K. In *Lecture Notes in Physics*; Marques, M. A. L., Ullrich, C. A., Nogueira, F., Rubio, A., Burke, K., Gross, E. K. U., Eds.; Springer-Verlag: Berlin, Heidelberg, Germany, 2006; Vol 706, pp 1−13.
(18) Maitra, N. T.; Burke, K.; Woodward, Chr. *Phys. Rev. Lett.* **2002**, *89*, 023002.
(19) Baer, R.; Kurzweil, Y.; Cederbaum, L. S. *Isr. J. Chem.* **2005**, *45*, 161.
(20) Kurzweil, Y.; Baer, R. *Phys. Rev. B* **2006**, *73*, 075413.
(21) Wijewardane, H. O.; Ullrich, C. A. *Phys. Rev. Lett.* **2005**, *95*, 086401.

(22) Castro, A.; Werschnik, J.; Gross, E. K. U. arxiv.org/1009.2241
(23) Shapiro, M.; Brumer, P. In *Principles of the Quantum Control of Molecular Processes*; Wiley: New York, 2003.
(24) Krotov, V. F. In *Global Methods in Optimal Control Theory*; Dekker: New York, 1996.
(25) Zhu, W.; Rabitz, H. *J. Chem. Phys.* **1998**, *109*, 385.
(26) Krause, P.; Klamroth, T.; Saalfrank, P. *J. Chem. Phys.* **2005**, *123*, 074105.
(27) Klamroth, T. *Phys. Rev. B* **2003**, *68*, 245421.
(28) Klamroth, T. *J. Chem. Phys.* **2006**, *124*, 144310.
(29) Klamroth, T.; Nest, M. *Phys. Chem. Chem. Phys.* **2009**, *11*, 349.
(30) Kronik, L.; Makmal, A.; Tiago, M. L.; Alemany, M. M. G.; Jain, M.; Huang, X.; Saad, Y.; Chelikowsky, J. R. *Phys. Status Solidi B* **2006**, *243*, 1063.
(31) Mundt, M. *J. Theor. Comput. Chem.* **2009**, *8*, 561.
(32) Troullier, N.; Martins, J. L. *Phys. Rev. B* **1991**, *43*, 1993 The core radii (in a_0) are as follows: Li, s(2.43), p(2.43); C, s(1.49), p(1.42); N, s(1.50), p(1.50), with Li(s), C(p), and N(p) as local components.
(33) Ceperley, D. M.; Alder, B. J. *Phys. Rev. Lett.* **1980**, *45*, 566.
(34) Perdew, J. P.; Zunger, A. *Phys. Rev. B* **1981**, *23*, 5048.
(35) Perdew, J. P.; Burke, K.; Ernzerhof, M. *Phys. Rev. Lett.* **1996**, *77*, 3865.
(36) Ernzerhof, M.; Scuseria, G. E. *J. Chem. Phys.* **1999**, *110*, 5029.
(37) Xu, X.; Goddard, W. A., III *Proc. Natl. Acad. Sci. U. S. A.* **2004**, *101*, 2673.
(38) Mundt, M.; Kümmel, S. *Phys. Rev. B* **2007**, *76*, 035413.
(39) Castro, A.; Marques, M. A. L.; Rubio, A. *J. Chem. Phys.* **2004**, *121*, 3425.
(40) Vosko, S. H.; Wilk, L.; Nusair, M. *Can. J. Phys.* **1980**, *58*, 1200.
(41) Frisch, M. J.; Trucks, G. W.; Schlegel, H. B.; Scuseria, G. E.; Robb, M. A.; Cheeseman, J. R.; Scalmani, G.; Barone, V.; Mennucci, B.; Petersson, G. A.; Nakatsuji, H.; Caricato, M.; Li, X.; Hratchian, H. P.; Izmaylov, A. F.; Bloino, J.; Zheng, G.; Sonnenberg, J. L.; Hada, M.; Ehara, M.; Toyota, K.; Fukuda, R.; Hasegawa, J.; Ishida, M.; Nakajima, T.; Honda, Y.; Kitao, O.; Nakai, H.; Vreven, T.; Montgomery, J. A., Jr.; Peralta, J. E.; Ogliaro, F.; Bearpark, M.; Heyd, J. J.; Brothers, E.; Kudin, K. N.; Staroverov, V. N.; Kobayashi, R.; Normand, J.; Raghavachari, K.; Rendell, A.; Burant, J. C.; Iyengar, S. S.; Tomasi, J.; Cossi, M.; Rega, N.; Millam, N. J.; Klene, M.; Knox, J. E.; Cross, J. B.; Bakken, V.; Adamo, C.; Jaramillo, J.; Gomperts, R.; Stratmann, R. E.; Yazyev, O.; Austin, A. J.; Cammi, R.; Pomelli, C.; Ochterski, J. W.; Martin, R. L.; Morokuma, K.; Zakrzewski, V. G.; Voth, G. A.; Salvador, P.; Dannenberg, J. J.; Dapprich, S.; Daniels, A. D.; Farkas, Ö.; Foresman, J. B.; Ortiz, J. V.; Cioslowski, J.; Fox, D. J. *GAUSSIAN09*; Gaussian, Wallingford, CT, 2009.
(42) Nest, M. *Chem. Phys.* **2010**, *370*, 119.
(43) Nest, M. *Int. J. Quantum Chem.* **2011**, *111*, 505.
(44) Werner, H.-J.; Knowles, P. J.; Lindh, R.; Manby, F. R.; Schütz, M.; Celani, P.; Korona, T.; Mitrushenkov, A.; Rauhut, G.; Adler, T. B.; Amos, R. D.; Bernhardsson, A.; Berning, A.; Cooper, D. L.; Deegan, M. J. O.; Dobbyn, A. J.; Eckert, F.; Goll, E.; Hampel, C.; Hetzer, G.; Hrenar, T.; Knizia, G.; Köppl, C.; Liu, Y.; Lloyd, A. W.; Mata, R. A.; May, A. J.; McNicholas, S. J.; Meyer, W.; Mura, M. E.; Nicklass, A. Palmieri, R.; Pflüger, K.; Pitzer, R.; Reiher, M.; Schumann, U.; Stoll, H.; Stone, A. J.; Tarroni, R.; Thorsteinsson, T.; Wang, M.; Wolf. A. *Molpro*, Version 2009.1, a package of ab initio programs; 2008.
(45) Hariharan, P. C.; Pople, J. A. *Theor. Chim. Acta* **1973**, *28*, 213.
(46) Tremblay, J. C.; Klamroth, T.; Saalfrank, P. *J. Chem. Phys.* **2008**, *129*, 084302.
(47) Klinkusch, S.; Saalfrank, P.; Klamroth, T. *J. Chem. Phys.* **2009**, *131*, 114304.
(48) Padmanaban, R.; Nest, M. *Chem. Phys. Lett.* **2008**, *463*, 263.
(49) Mundt, M.; Tannor, D. J. *New J. Phys.* **2009**, *11*, 105038.
(50) Nest, M.; Remale, F.; Levine, R. D. *New. J. Phys.* **2008**, *10*, 025019.
(51) Plötner, J.; Tozer, D. J.; Dreuw, A. *J. Chem. Theor. Comput.* **2010**, *6*, 2315.
(52) Peach, M. J. G.; Benfield, P.; Helgaker, T.; Tozer, D. J. *J. Chem. Phys.* **2008**, *128*, 044118.
(53) Fuks, J. I.; Helbig, A.; Tokatly, I. V.; Rubio, A. arxiv.org/abs/1101.2880
(54) Ruggenthaler, M.; Bauer, D. *Phys. Rev. Lett.* **2009**, *102*, 233001.